

Computational study of the Dehydrogenation Effect of Dopant Ti on Nanostructured NaAlH₄ Cluster

Xiaogang Tong and Hongshan Chen^{a)}

College of Physics and Electronic Engineering, Northwest Normal University, Lanzhou 730070, China

Abstract

Employing the evolutionary algorithm combined with density functional theory and perturbation theory model, we investigate the geometric and electronic structures of pure and Titanium-doped Na₄Al₄H₁₆ cluster to demonstrate the effect of dopant Ti on the dehydrogenation properties of the nanostructured NaAlH₄. The result shows the Ti-doped Na₄Al₄H₁₆ clusters are more stable thermodynamically, but the average dehydrogenation enthalpies and the energy barriers for H₂ desorption are significantly decreased. Doping of Ti weakens the Al-H bond, reduces the dehydrogenation temperatures, and the dehydrogenation performance of the NaAlH₄ nanocluster is conspicuously promoted.

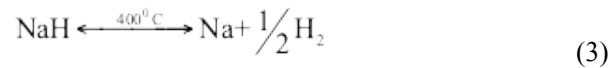
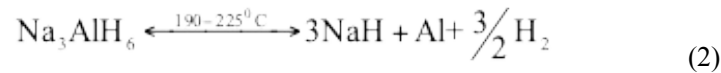
Keywords: Hydrogen storage, Nanocluster, Stability, Electronic structure, Desorption energy barrier, Dehydrogenation enthalpy.

1 Introduction

The economy based on traditional energy has brought many new challenges to human society, such as pollution and irreversible climate change caused by over-exploitation, drilling and increasing greenhouse gases. Hydrogen has proven to be an attractive alternative energy carrier [1,2], especially for hydrogen polymer electrolyte membrane (PEM) fuel cells [3]. Nowadays, hydrogen-powered vehicles and fuel cell vehicles (HFCV) are available on the market, but the unsatisfactory hydrogen storage performance of materials limits the wide application of hydrogen energy economy in commercial applications. Solid materials are considered to be potential hydrogen storage materials [4], and the excellent one should meet a series of standards set by U.S. Department of Energy (DoE). The weight capacity of hydrogen should reach or exceed 7.5 wt%, the number of reversible cycles should be at least 1500, and the hydrogen is released below 85°C so that the operation is practical. The hydrogen release rate required is as high as 2g H₂ s⁻¹ and the absorption rate of is also fast enough (about 15 g H₂ s⁻¹). Many materials have been tested for hydrogen storage applications in past, and a plenty of strategies, including changing the morphology of hydride particles [5], mechanical strain [6], entropy effect [7], and dopants or other chemical additives, have been considered to improve their hydrogen storage performance [8,9].

^{a)} Author to whom correspondence should be addressed. Email: chenhs2021@163.com

The complex hydride NaAlH₄ has been shown a prototypical candidate for hydrogen storage material due to its high weight density of hydrogen storage, low cost and mild thermodynamic properties [10,11]. The NaAlH₄ liberate 7.4 wt% hydrogen via the follow three-step reaction [12,13]



The hydrogen liberation density for the three-step reaction (1), (2) and (3) is 3.7wt%, 1.9wt% and 1.8wt%, and the dehydrogenation enthalpy ΔH is 40.9 kJmol⁻¹, 15.6 kJmol⁻¹ and 20 kJmol⁻¹ respectively. While the high desorption temperature, poor reversibility and slow dehydrogenation/rehydrogenation kinetics hinder its practical application widely for a long time because of the intricate reaction pathways and involved myriad intermediates.

Adding a suitable catalyst can greatly reduce the energy barrier, make the material reversible, and speed up the reaction rates under moderate conditions. Since Bogdanovic reported firstly that the Ti-based catalysts can effectively improve the hydrogen storage performance of NaAlH₄ [14], various catalysts including transition metals, rare-earth metals and carbon-based materials, have been studied to improve its hydrogen storage properties[15-19], the results shows most transition metal compounds have a good catalytic effect, and the titanium compounds have still been proven the most effective catalyst for increasing dehydrogenation and rehydrogenation rate till now. Identifying the nature of the catalyst Ti is quite important for understanding mechanism of hydrogen release in doped NaAlH₄, in 2011, Frankcombe provided a detailed review of the Ti catalytic mechanism for NaAlH₄ [20], these include the mechanisms of mobile species, role of mobile vacancies, altering the fermi level, destabilizing Al-H bond, nucleation/phase growth, zipper model, mixed effect models and so forth. As we all know, the highly stable [AlH₄] group is the main factor that controll the dehydrogenation reaction of NaAlH₄. Tremendous theoretical investigation have been reported to clarify the effect of Ti on destabilizing the AlH₄ unit [21-24]. Using Ab initio molecular dynamics simulations, Iniguez and Yildirim speculate that Ti prefer to remain on the surface and is replaced by Na energetically[21], Ti is surrounded by a plenty of H atoms which can transport between the Ti and the Al atoms freely and continuously, this cause to the weakening of the Al-H bonding, and help to the H₂ release and formation, therefore, the reaction kinetics of the NaAlH₄ is enhanced. Dathara and Mainardi predict that Ti can extract

hydrogen atoms from the accessible AlH_4 or AlH_3 groups, the Ti-H bonds newly formed are easily broken compared with those in the AlH_4 or AlH_3 groups [22]. Du et al. propose that charge transfer to the AlH_4 anion is suppressed owing to the surface defects, which can lead to effectively promoting the H_2 recycling performance of NaAlH_4 [23]. Wang et al. suggest that a local electrostatic attraction is created between Ti^{n+} ($n < 2$) and a specific H^- in $[\text{AlH}_4]^-$ when the two phases are close sufficiently, this is a mechanism responsible for the improved dehydrogenation reactions of doped NaAlH_4 . [25] The addition of titanium-based catalysts is believed to be beneficial to promote the nucleation of dehydrogenation products [26], Kang et al. noted that the TiH_2 particles always remain near the center of the segregated Al-rich particles in the cycling of H_2 [27], hydride TiH_2 is predicted to a nucleation center for Al since the favorable lattice matching between Al and TiH_2 , thus the local growth in the dehydrogenation process is induced energetically.

Nanostructuring of the metal hydrides is a transformative approach for hydrogen storage, Nanosized complex hydrides NaAlH_4 have proved to be promising candidates for hydrogen storage application, which has attracted extensive attention in the past decade [28-30]. The hydrides at nanosize have a high surface area and increased surface energy, which could significantly promote thermodynamic or kinetic properties of hydrogen adsorption; Nanosizing can affect the interfaces of different material phases and produce some forms of lattice deformation or distortion that is beneficial for cycling; Furthermore, nanoconfinement can fundamentally change the properties of materials through chemical or electronic interaction with confinement media, or through mechanical confinement stress. For the complex hydrides NaAlH_4 , due to the high lattice enthalpy and strong ionic and covalent bonding, the operating temperature is too high. A main goal of nanoconfinement is to destabilize the hydride so that reducing the reaction enthalpy, thus make the operating temperature within a reasonable range for practical applications. Nanosizing can significantly reduce diffusion lengths, facilitate chemical kinetics and nucleation as well as alter reaction pathways, for example, the desorption barriers of H_2 from NaAlH_4 are noticed to depend on the size of cluster or particle considerably [31-33].

Though a plenty of research works have been carried out to improve the hydrogen- storage properties of this complex, the general consensus on understanding the catalytic mechanism have not been thoroughly reached, the most important is that the research results achieved about NaAlH_4 material are not very satisfactory for onboard applications. In this paper, we aim at Ti-doped NaAlH_4 nanoclusters as model systems to study their geometric and electronic structures so as to analyze the influence effect of Ti on the dehydrogenation properties of the nanostructured NaAlH_4 . Even though the size and environmental conditions of the gas-phase clusters

are significantly different from those of the bulk clusters, they can be employed to reveal complex nature of the chemical bonding process, and provide insight into the characteristics of hydrogen storage for NaAlH₄ bulk material.

2 Computational methods

The Universal Structures Prediction Evolutionary Xtallography (USPEX) [34] implemented by the VASP [35] software package is adopted to search globally the low-energy structures of pure and doped (NaAlH₄)₄ clusters. The initial generation with 20 structures produced randomly is optimized through genetic, replacement and mutation operators. If the best structure does not change within the 30th generation, then the iteration stops. The projector augmented wave (PAW) pseudopotentials and the Perdew-Burke-Ernzerhof (PBE) exchange-correlation functional in generalized gradient approximation [36,37] is employed, the cutoff energy for the plane wave expansion is 500 eV. The convergence criteria for the energy and the maximum force are respectively 10⁻⁵ eV and 10⁻³ eV/Å. The low-energy structures obtained by USPEX are further optimized through density functional method B3LYP and double hybrid method B2PLYPD [38,39] using the basis of triplet- ζ set 6-311+G(d, p) with diffuse and polarization functions, without any symmetry restriction. The B2PLYPD method is employed to evaluate the reliability of the B3LYP-D3 result as its good consideration for the correlation energy. Transition state (TS) search was conducted through performing partial optimization and further confirmed by the quadratic synchronous transit approach (QST2) methods [40], Vibrational frequencies are computed to make sure that the optimized structures are transition states (TSs) or energy minima, the computations of this parts are completed using Gaussian 09 program[41].

3 Results and discussions

3.1 Geometric structures and bond length

The first four low-energy structures of the pure Na₄AlH₁₆ cluster further optimized at B3LYP/6-311+G(D, P) level are shown in Fig. 1, each of them contains four AlH₄ units, Al bind with Na through H bridges and there exist a terminal H_t atom for most Al atoms, and Al are seven or six coordinated. For the lowest-energy isomer Na₄AlH₁₆-a, the four Al atoms forms triangular pyramid, the four Na atoms sit above the four side-faces of the pyramid, and has the C_{3v} symmetry, this is consistent with the result reported previously[42]. The Na₄AlH₁₆-b forms a Al-Na network structure similar to a distorted curve surface. The Na₄AlH₁₆-c looks like a bug, one H atom break away from a AlH₄ unit and bond three Na atom. The Na₄AlH₁₆-d forms approximate square network with C_{4v} symmetry, the four Al atoms are located at the vertexes.

Three doping schemes are considered, that is substitution of Ti for a Al or Na atom, and direct doping of Ti in the $\text{Na}_4\text{Al}_4\text{H}_{16}$ cluster. Fig. 2 illustrates the low-energy isomers of Ti-doped clusters of $\text{Na}_4\text{Al}_4\text{TiH}_{16}$, $\text{Na}_3\text{TiAl}_4\text{H}_{16}$ and $\text{Na}_4\text{Al}_3\text{TiH}_{16}$ globally searched. Doping of Ti makes the structure of $\text{Na}_4\text{Al}_4\text{H}_{16}$ changed considerably, the structures doesn't appear certain symmetry. The Ti atom is roughly located at the center of the cluster and is surrounded by seven hydrogen for each structure, Ti captures hydrogen from the AlH_4 group of the Ti-doped $\text{Na}_4\text{Al}_4\text{H}_{16}$ cluster, this result in only two or three hydrogen remained on certain Al atoms. Ti bind with each of the Al or Na through H bridges for all the isomers. There are four kind of bridge H_b atoms, that is the cases of Al- H_b -Na, Ti- H_b -Al, Ti- H_b -Na, and H_b connecting together with three atoms of Ti, Al and Na (occasionally), thus there are two types of Ti- H_b bond. It is found the number of terminal H_t is reduced to two or three for the $\text{Na}_4\text{Al}_4\text{TiH}_{16}$ and $\text{Na}_3\text{TiAl}_4\text{H}_{16}$, and there is no H_t atom for $\text{Na}_4\text{Al}_3\text{TiH}_{16}$ case. What is particularly striking for the $\text{Na}_4\text{Al}_3\text{TiH}_{16}$ is that two hydrogen atoms have been desorbed and is adsorbed on the Na atoms in molecular form, the calculated adsorption energy of H_2 molecule is only -0.045 eV.

The average bond length for the lowest-energy isomers of these clusters are listed in Table 1. In cluster NaAlH_4 -a, the four Al-Al distance of the bevel edge is 4.78 Å, and the three Al-Al distance of the bottom is 5.61 Å. The values of the bond length of Al-H (1.64 Å), Na-H (2.22 Å) and Al-Na (3.47 Å) are comparable to those of the NaAlH_4 crystal at room temperature [10]. Compared to the pure $\text{Na}_4\text{TiAl}_4\text{H}_{16}$, the bond length Al- H_t changes very little in the $\text{Na}_3\text{TiAl}_4\text{H}_{16}$ and $\text{Na}_4\text{Al}_4\text{TiH}_{16}$, and there is no Al- H_t bond in $\text{Na}_4\text{Al}_3\text{TiH}_{16}$; The Al- H_b bond length in the bridges of Al- H_b -Na are elongated a little, while those in the Al- H_b -Ti are stretched considerably compared with pure $\text{Na}_4\text{Al}_4\text{H}_{16}$ cluster, the enlarged Al-H bonds can be broken easily and help to the releasing of H atoms. The Ti- H_b bond length in Ti- H_b -Al bridges are longer than those in Ti- H_b -Na. The average bond length of Ti-Al or Na-H don't differ very much in three doped cases, the Al-Na in Ti-doped clusters becomes shorter than that in pure $\text{Na}_4\text{TiAl}_4\text{H}_{16}$ respectively. It is noticed that the three Ti-Al bond length in $\text{Na}_4\text{Al}_3\text{TiH}_{16}$ are all equal and 2.81 Å, and is comparable to the magnitude in Al_3Ti compound.

3.2 The stabilities

The thermodynamic stability of cluster can be judged validly by binding energy E_b , it is defined as the energy difference between cluster and the constituent atoms, the E_b of the $\text{Al}_k\text{Na}_l\text{H}_{16}\text{Ti}$ cluster is expressed as the follow:

$$E_b = E(\text{Al}_k\text{Na}_l\text{H}_{16}\text{Ti}) - kE(\text{Al}) - lE(\text{Na}) - E(\text{Ti}) - 16E(\text{H})$$

Where $E(\text{Al}_k\text{Na}_l\text{H}_{16}\text{Ti})$ is the energy of the cluster, $E(\text{Al})$, $E(\text{Na})$, $E(\text{Ti})$ and $E(\text{H})$ is the energy of the constituent atoms, respectively. The binding energy calculated by

B3LYP/6-311+G(d,p) and B2PLYPD/6-311+G(d, p) model are listed in Table 2, the magnitudes calculated by B2PLYPD is slightly higher than that by B3LYP method but the trend is consistent. The magnitudes of E_b for Ti-doped cases are larger than that of pure cluster $\text{Na}_4\text{Al}_4\text{H}_{16}$, which indicates that doping of Ti makes the clusters more stable thermodynamically. Moreover, the E_b is dependent on the rate of Al and Na atomic numbers, the E_b of the $\text{Na}_4\text{Al}_4\text{TiH}_{16}$ is the largest, and the $\text{Na}_4\text{Al}_3\text{TiH}_{16}$ is the smallest.

The chemical stability can be measured by HOMO-LUMO energy gap E_g , Table 2 also lists the energy gap, It is noticed that the magnitudes of E_g value of Ti-doped clusters are smaller than that of the pure $\text{Na}_4\text{Al}_4\text{H}_{16}$, this suggests the chemical stability of the doped clusters becomes low.

3.3 Dehydrogenation properties

3.3.1 Dehydrogenation enthalpy

One of the important thermodynamic parameter for hydrogen storage materials is dehydrogenation enthalpy that determines the heat of dehydrogenation reaction and affects the temperature of reversible processes. The dehydrogenation enthalpy ΔH_a of $E(\text{Al}_k\text{Na}_l\text{H}_{16}\text{Ti})$ is calculated using the follow equation:

$$\Delta H = E(\text{Al}_k\text{Na}_l\text{Ti}) + nE(\text{H}_2) - E(\text{Al}_k\text{Na}_l\text{H}_{2n}\text{Ti})/n$$

Where $E(\text{Al}_k\text{Na}_l\text{H}_{2n}\text{Ti})$, $E(\text{Al}_k\text{Na}_l\text{Ti})$ and $E(\text{H}_2)$ are the total energy of $\text{Al}_k\text{Na}_l\text{H}_{16}\text{Ti}$, $\text{Al}_k\text{Na}_l\text{Ti}$ clusters, and free H_2 molecule, respectively. The $n=8$ and 1 corresponds to the average dehydrogenation energy ΔH_a of $\text{Al}_k\text{Na}_l\text{H}_{16}\text{Ti}$ and the dehydrogenation energy ΔH_l of removing the last two hydrogens in $\text{Al}_k\text{Na}_l\text{H}_2\text{Ti}$, respectively. The magnitudes of average ΔH_a for the whole clusters and ΔH_l for only two H atoms remained are listed in Table 2. The results calculated by B3LYP/6-311+G(d,p) is slightly lower than that by B2PLYPD/6-311+G(d,p). The dehydrogenation enthalpies ΔH_a becomes low compared to the pure $\text{Al}_4\text{Na}_4\text{H}_{16}$, and the value is related to the rate of Al and Na atomic numbers, Doping of Ti decrease the dehydrogenation temperature and is favorable for the dehydrogenation. That magnitudes of ΔH_l is higher than that of ΔH_a shows that the dehydrogenation properties of the hydride is related to the content of Ti, Ti-doping at low titanium content favours the initial dehydrogenation of AlNaH_4 , and the dehydrogenation becomes more difficult as the reaction progresses, this is consistent with the fact that the second and third steps of the dehydrogenation reactions of the bulk AlNaH_4 can only be achieved at higher temperatures. It is found that the value ΔH_a 1.18 eV/ H_2 (113.28 kJ/ H_2) of pure $\text{Al}_4\text{Na}_4\text{H}_{16}$ clusters is close to the experimental result of 118.9 kJ/ H_2 , the apparent activation energies for the first step of dehydrogenation reaction of the bulk AlNaH_4 [43].

3.3.2 Energy barriers for H_2 desorption

The energy barrier of dissociation for H₂ molecule is a most important factor to determine dynamic properties of hydrogen storage materials, to further explore the influence of the Ti atom on the dehydrogenation kinetics of Al₄Na₄H₁₆ clusters, we studied the desorption processes of H₂ molecule for the pure Na₄Al₄H₁₆ and doped Na₄Al₄H₁₆Ti and Na₃TiAl₄H₁₆ clusters. We select to remove a pair of neighbor H atoms (one terminal and one bridge) binding with Al nearest to Ti.

The H₂ desorption process is investigated by performing partial optimization at different reduced H-H distance and computing the energy of the cluster at each desorption step. The structure distorts slightly and the total energy of the system increases slowly at the beginning of the H-H bond length is shortened, the energy reaches the highest value around certain H-H distance and then lowers gradually. The transition state (TS) is obtained by carrying out the optimization of transition state for the geometry with the highest energy, Then we studied the dissociation process using the reaction path following algorithm, that is intrinsic reaction coordinate (IRC) [44, 45], to get the energy curve along the desorption path from initial state to H₂ desorbed structures.

The picture of (1), (2), (3) in Fig. 3 illustrate the energy curves along the H₂ desorption steps from clusters of Al₄Na₄H₁₆, Al₄Na₄H₁₆Ti, Al₄Na₃TiH₁₆, respectively. The energies are given relative to that of the H₂ desorbed structures and a free H₂ molecule. The dehydrogenation energy barriers are also listed in Table 2. The magnitude for pure Al₄Na₄H₁₆ is 2.46 eV at B3LYP/6-311+G(d,p) level, while the energy barriers on Al₄Na₄H₁₆Ti and Al₄Na₃TiH₁₆ are 1.93 eV and 2.31 eV, which are obviously lower than that on the pure cluster. The Ti-doping is favorable for the improvement of the dehydrogenation kinetics of the Al₄Na₄H₁₆ clusters, the hydrogens can be easily desorbed.

3.4 The electronic structures

The above discussions show that the dehydrogenation performance is considerably improved in Ti-doped Al₄Na₄H₁₆ clusters. In order to have a clearer understanding of the enhanced dehydrogenation mechanism, we studied the electronic structure of the systems in terms of Charge Population Method, the Electron Localization Function (ELF) and the Crystal Orbital Hamilton Population (COHP).

3.4.1 Charge population analysis

Since the electronegativity between Na or Al or Ti atoms and H atoms is quite different, it can be considered that Na-H, Al-H and Ti-H bonds are strongly polarized, so charge distribution plays an important role in bonding strength. Here we adopt the natural bond orbitals (NBO) method [46], it is widely used and provide satisfactory results. Table 3 list the calculated NBO charges on Al/Na/H/Ti atoms. Compared with the pure Na₄Al₄H₁₆, the corresponding charges on Al/Na for doped cases is increased,

so the Al/Na atoms lost more electrons. Na atoms transfer most of their 3s electrons and exist nearly as +1 cations, the charges change on Al atoms is more than the pure case. The charges (magnitudes) on terminal H_t and bridge H_b atoms are all decreased, so the H obtains less electrons, this will lead to Al-H bond weakening. Ti obtain electrons as Ti is negatively charged, and the magnitude on Ti for Na₄Al₄H₁₆Ti case is the largest. The redistribution of the charge imply that the bonding nature between the atoms in Na₄Al₄H₁₆ clusters have been changed for the doped cases.

3.4.2 Electron localization function analysis

In order to understand the bonding characteristics visually, we the electron localization function (ELF) is analyzed [47, 48], which is defined as the follow:

$$ELF = \left[1 + \left(\frac{\frac{1}{2} \sum_i |\nabla \phi_i|^2 - \frac{1}{8} \frac{|\nabla \rho|^2}{\rho}}{\frac{3}{10} (3\pi^2)^{2/3} \rho^{5/3}} \right)^2 \right]^{-1}$$

Where ρ and $\nabla \rho$ is total electron density and its gradient, respectively, and

$\sum_i |\nabla \phi_i|^2$ is kinetic energy density. ELF uses the probability of electron pairs to reflect effectively the bonding properties, the spatial distribution of the local maxima of ELF (defined as the localization attractors) can describe characterization of covalency versus ionicity. Bonding attractors are located between core attractors (around the nucleus) and describe covalent interactions. The large attractors means a pair of highly localized electrons, the normalized value 1.0 stand for perfect localization, the value 0.5 means the homogeneous electron gas and small values corresponds to low electron densities. The picture (1), (2), (3) and (4) in Fig. 4 shows the ELF contour lines on a specific plane of the four lowest-energy isomers Na₄Al₄H₁₆-a, Na₄Al₄TiH₁₆-a, Na₃TiAl₄H₁₆-a and Na₄Al₃TiH₁₆-a, respectively.

For picture (1), the distribution of the ELF obviously indicates that Al and H form a unit, the valence electrons are basically resided around the hydrogen nuclei, and the Na⁺ cores is not enclosed by the valence electrons, this bonding property is similar to the case in the complex hydride NaAlH₄. The electrons density of H atoms near Al or Na atoms is larger, the localization attractors between Al and H is 0.05, the Al-H is covalent bond, the Na and H forms ionic bond, the ELF also reveal that Al interacts with Na through hydrogen bridges.

For the (2), (3) and (4) of Ti-contained, the distributions of the valence electrons of Ti atoms are distorted, especially the Na-replaced case in picture (3), Ti interacts with surrounding atoms. The attractors between Ti and Al is from 0.35 to 0.7, this

shows the nature of Ti-Al bond will change slightly in different systems, but it is basically covalent with ionic characteristics. The localized attractors between Ti and H is about 0.15, combined charge analysis, Ti-H bond accords with the characteristics of covalence. The formed Ti-Al and Ti-H changes the electronic structure of the AlH_4 groups in pure $\text{Na}_4\text{Al}_4\text{H}_{16}$ cluster and influence the Al-H bond strength. The ELF of Na atoms still appears an independent parts in doped cases.

3.4.3 The crystal orbital Hamilton population (COHP)

The above discussions imply that the Al-H interactions are weakened in a certain extent. In order to quantitatively examine the bond strength between related atoms, we calculated the energy integral of the Crystal Orbital Hamilton Population (COHP) [49-5], the energy integral of the COHP indicates strength of covalent bond quantitatively, and it has proved to be a reliable and efficient bond-detecting tool for crystals or clusters, The one-electron wave functions $\psi_i(r)$ of a cluster or the extended crystal can be formed by a linear combination of atomic centered orbitals $\varphi_\mu(r)$,

$$\psi_i(r) = \sum_A \sum_{\mu=1(\mu \in A)}^n C_{\mu i} \varphi_\mu(r)$$

Where $C_{\mu i}$ is the mixing coefficient. Solving this Schrödinger equation using the variational principle, one can obtain the follow secular determinant:

$$\sum_{A,B} \sum_{\mu,\nu} C_{\mu i}^i C_{\nu i} H_{\mu\nu} - \sum_{A,B} \sum_{\mu,\nu} C_{\mu i}^i C_{\nu i} S_{\mu\nu} E_i = 0$$

Where $H_{\mu\nu} = \langle \varphi_\mu | \hat{H} | \varphi_\nu \rangle$ and $S_{\mu\nu} = \langle \varphi_\mu | \varphi_\nu \rangle$ are Hamiltonian and overlap

matrices. The summation of the one particle energy is so called COHP:

$$\sum_i f_i E_i = \sum_{A,B} \sum_{\mu,\nu} H_{\mu\nu} \sum_i f_i C_{\mu i}^* C_{\nu i} = \sum_{A,B} \sum_{\mu,\nu} H_{\mu\nu} P_{\mu\nu}(E) = \sum_{A,B} \sum_{\mu,\nu} \text{COHP}_{\mu\nu}(E)$$

Where f_i is the occupation number, $H_{\mu\nu} = \langle \varphi_\mu | H | \varphi_\nu \rangle$ is the Hamiltonian matrices and $P_{\mu\nu}(E)$ is the population densities. COHP shows the contribution of an atom or a chemical bond to the one-particle energies. In particular the off-site terms ($\mu \in A, \nu \in B$ and $A \neq B$) can be interpreted as a measure for the strength of covalent bonding. When replacing the $S_{\mu\nu}$ in the overlap population-weighted DOS with the

$H_{\mu\nu}$, the Bonding and anti-bonding are indicated by the negative and positive values of COHP.

The $-I_{\text{COHPs}}$, which is the COHP values integrated over the occupied states, are listed in Table 4. It shows the Al-H covalent interactions becomes obviously weak in the Ti-doped structures, the weakened Al-H bond is mainly responsible for the enhanced dehydrogenation performance. The magnitude $-I_{\text{COHPs}}$ of Ti-Al bond is from 0.68 to 0.99 eV shows the complexity of the bonding, while it is mainly covalent. The $-I_{\text{COHP}}$ values for Ti-H bond is from 1.08 to 1.51 eV, which further indicates that the Ti-H bonding is basically covalent. The formed covalent Ti-H and Ti-Al bond weakens the strength of Al-H bond in Ti-doped cluster. The $-I_{\text{COHP}}$ values for the Na-H and Na-Al bond in doped cases is larger, this reflects their ionic interactions becomes weak.

4 Conclusions

The low-energy isomers of pure and Ti-doped $\text{Al}_4\text{Na}_4\text{H}_{16}$ clusters are determined by the evolutionary algorithm combined with the density functional method to investigate the influence effect of dopant Ti on the dehydrogenation properties for the $\text{Na}_4\text{Al}_4\text{H}_{16}$ nanocluster. The Calculation results are summarized as the follow: (1) There exist AlH_4 groups in the isomers of pure $\text{Al}_4\text{Na}_4\text{H}_{16}$ cluster, which is similar to the structure of the complex hydride AlNaH_4 . In doped clusters, Ti atoms are generally located at the center of the clusters, Al or Na atoms connect with Ti atoms through H bridges, and the Al-H_b bond length are obviously stretched. (2) The magnitudes of binding energy shows the thermodynamic stability of doped clusters are enhanced compared with the pure case, while the chemical stability becomes weak. (3) The average dehydrogenation energies of the doped cluster are decreased, the temperatures of entire dehydrogenation are reduced. (4) The energy barriers to desorb H_2 molecules from the doped clusters are obviously lower, the dynamics properties of dehydrogenation is greatly enhanced. (5) The NBO charges shows that the Al and Na atoms further lost electrons and the charges on the bridge H atoms become considerably smaller for the Ti-doped clusters, Ti atom is negatively charged. (6) The ELF shows the Ti-H and Ti-Al bond is formed in doped systems, which can cause the related Al-H bond strength changed. (7) The COHP analysis indicates that the Al-H bond strength is weakened considerably after doped, the degree of weakening is different for different doping situations at nanoscale. The present results indicates that the weakened Al-H bonds caused by Ti-Al or/and Ti-H interaction is mainly responsible for the improved dehydrogenation performance, Ti-doped nanostructured NaAlH_4 is promising hydrogen storage materials.

Acknowledgment

This work is financially supported by the National Natural Science Foundation of China (Grant No. 11664034).

References

- [1] Chu, S.; Majumdar, A. Opportunities and Challenges for a Sustainable Energy Future. *Nature*. 2012; 488: 294-303.
- [2] Kasper T. Møller, Torben R. Jensen, Etsuo Akiba, Hai-wen Li. Hydrogen-A sustainable energy carrier. *Progress in Natural Science: Materials International*. 2017; 27: 34–40.
- [3] Wee, J. H. Applications of Proton Exchange Membrane Fuel Cell Systems. *Renewable Sustainable Energy Rev*. 2007; 11: 1720–1738.
- [4] Schlapbach L and Züttel A. Hydrogen-storage materials for mobile applications. *Nature*. 2001; 414: 353-358.
- [5] Bérubé, V.; Radtke, G.; Dresselhaus, M.; Chen, G. Size Effects on the Hydrogen Storage Properties of Nanostructured Metal Hydrides: A Review. *Int. J. Energy Res*. 2007; 31: 637–663.
- [6] Benzidi, H.; Lakhal, M.; Benyoussef, A.; Hamedoun, M.; Loulidi, M.; El kenz, A.; Mounkachi, O. First Principle Study of Strain Effect on Structural and Dehydrogenation Properties of Complex Hydride LiBH_4 . *Int. J. Hydrogen Energy*. 2017; 42: 19481–19486.
- [7] Berube, V.; Dresselhaus, M. S.; Chen, G. Entropy Stabilization of Deformed Regions Characterized by an Excess Volume for Hydrogen Storage Applications. *Int. J. Hydrogen Energy*. 2009; 34: 1862–1872.
- [8] Churchard, A. J.; Banach, E.; Borgschulte, A.; Caputo, R.; et al. A Multifaceted Approach to Hydrogen Storage. *Phys. Chem. Chem. Phys*. 2011, 13, 16955–16972.
- [9] Kan, H. M.; Zhang, N.; Wang, X. Y.; Sun, H. Recent Advances in Hydrogen Storage Materials. *Adv. Mater. Res*. 2012; 512–515:1438– 1441.
- [10] Shin-ichi Orimo, Yuko Nakamori, Jennifer R. Eliseo, Andreas Züttel, and Craig M. Jensen. Complex Hydrides for Hydrogen Storage. *Chem. Rev*. 2007; 107: 4111-4132.
- [11] Yongfeng Liu, Zhuanghe Ren, Xin Zhang, Ni Jian, Yaxiong Yang, Mingxia Gao, and Hongge Pan. Development of Catalyst-Enhanced Sodium Alanate as an Advanced Hydrogen-Storage Material for Mobile Applications. *Energy Technol*. 2018; 6: 487 – 500.
- [12] Mao, J.; Guo, Z.; Leng, H.; Wu, Z.; Guo, Y.; Yu, X.; Liu, H. Reversible hydrogen storage in destabilized $\text{LiAlH}_4\text{-MgH}_2\text{-LiBH}_4$ ternary-hydride system doped with TiF_3 . *J. Phys. Chem. C* 2010; 26: 11643–11649.
- [13] Nakagawa, Y.; Ikarashi, Y.; Isobe, S.; Hino, S.; Ohnuki, S. Ammonia borane–metal alanate composites: Hydrogen desorption properties and decomposition processes. *RSC Adv*. 2014; 4: 20626–20631.
- [14] Bogdanovic, B.; Schwickardi, M. Ti-Doped Alkali Metal Aluminium Hydrides as Potential Novel Reversible Hydrogen Storage Materials. *J. Alloys Compd*. 1997; 253:1–9.
- [15] X. Zhang, Y. Liu, K. Wang, M. Gao, H. Pan. Remarkably improved hydrogen storage properties of nanocrystalline TiO_2 -modified NaAlH_4 and evolution of Ti-containing species during dehydrogenation/hydrogenation. *Nano Res*. 2015; 8(2): 533–545.
- [16] P. Wang, X. D. Kang, H. M. Cheng. Exploration of the Nature of Active Ti Species in Metallic Ti-Doped NaAlH_4 . *J. Phys. Chem. B*. 2005; 109: 20131–20136.

- [17] Fan X, Xiao X, Chen L, et al. Enhanced hydriding–dehydriding performance of CeAl₂-doped NaAlH₄ and the evolution of Ce-containing species in the cycling. *J. Phys. Chem. C*. 2011; 115(5): 2537-2543.
- [18] J. Hu, S. Ren, R. Witter, M. Fichtner, *Adv. Energy Mater.* 2012, 2, 560–568.
- [19] V. P. Balema, L. Balema. Missing pieces of the puzzle or about some unresolved issues in solid state chemistry of alkali metal aluminohydrides. *Phys.Chem.Chem. Phys.* 2005; 7:1310 – 1314.
- [20] T. J. Frankcombe. Proposed Mechanisms for the Catalytic Activity of Ti in NaAlH₄. *Chem. Rev.* 2012; 112: 2164–2178
- [21] J. Iniguez, T. Yildirim. First-principles study of Ti-doped sodium alanate surfaces. *Appl. Phys. Lett.* 2005; 86: 103109.
- [22] G. K. P. Dathara, D. S. Mainardi. Structure and dynamics of Ti–Al–H compounds in Ti-doped NaAlH₄. *Mol. Simul.* 2008, 34, 201–210.
- [23] A. J. Du, S. C. Smith, G. Q. Lu. Role of charge in destabilizing AlH₄ and BH₄ complex anions for hydrogen storage applications: Ab initio density functional calculations. *Phys. Rev. B*. 2006; 74: 193405.
- [24] G. Miceli, M. Guzzo, C. Cucinotta, M. Bernasconi. First Principles Study of Hydrogen Desorption from the NaAlH₄ Surface Doped by Ti Clusters. *J. Phys. Chem. C*. 2012; 116 (6): 4311–4315.
- [25] P. Wang, X. D. Kang, H. M. Cheng. Exploration of the Nature of Active Ti Species in Metallic Ti-Doped NaAlH₄. *J. Phys. Chem. B*. 2005; 109 (43): 20131–20136.
- [26] K. J. Michel, V. Ozolin,s. Theory of mass transport in sodium alanate. *J. Mater. Chem. A*. 2014; 2: 4438–4448.
- [27] X.-D. Kang, P. Wang, H.-M. Cheng. Electron microscopy study of Ti-doped sodium aluminum hydride prepared by mechanical milling NaH/AlNaH/Al with Ti powder. *J. Appl. Phys.* 2006; 100: 034914.
- [28] Schneemann A, White J L, Kang S, et al. Nanostructured Metal Hydrides for Hydrogen Storage. *Chemical Reviews*. 2018; 118(22): 10775-10839
- [29] Qiwen Lai, Ting Wang, Yahui Sun, and Kondo-François Aguey-Zinsou. Rational Design of Nanosized Light Elements for Hydrogen Storage: Classes, Synthesis, Characterization, and Properties. *Adv. Mater. Technol.* 2018; 1700298
- [30] Miriam Rueda, Luis Miguel Sanz-Moral, Ángel Martín. Innovative methods to enhance the properties of solid hydrogen storage materials based on hydrides through nanoconfinement: A review. *The Journal of Supercritical Fluids*. 2018; 141: 198-217.
- [31] Nielsen, T. K.; Javadian, P.; Polanski, M.; Besenbacher, F.; Bystrycki, J.; Skibsted, J.; Jensen, T. R. Nanoconfined NaAlH₄: Prolific Effects from Increased Surface Area and Pore Volume. *Nanoscale*. 2014; 6: 599–607.
- [32] Bhakta, R. K.; Maharrey, S.; Stavila, V.; Highley, A.; Alam, T.; Majzoub, E.; Allendorf, M. Thermodynamics and Kinetics of NaAlH₄ Nanocluster Decomposition. *Phys. Chem. Chem. Phys.* 2012; 14: 8160–8169.
- [33] Stavila, V.; Bhakta, R. K.; Alam, T. M.; Majzoub, E. H.; Allendorf, M. D. Reversible Hydrogen Storage by NaAlH₄ Confined within a Titanium-Functionalized MOF-74(Mg) Nanoreactor. *ACS Nano*. 2012; 6: 9807–9817.

- [34] Oganov AR, Lyakhov AO, Valle M. How evolutionary crystal structure prediction works-and why. *Accounts Chem Res.* 2011; 44: 227-37.
- [35] Kresse G, Furthmuller J. Efficient iterative schemes for ab initio total-energy calculations using a plane-wave basis set. *Phys Rev B.* 1996; 54:11169-86.
- [36] Kresse G, Joubert D. From ultrasoft pseudopotentials to the projector augmented-wave method. *Phys Rev B.* 1999; 59:1758-75.
- [37] Perdew JP, Burke K, Ernzerhof M. Generalized gradient approximation made simple. *Phys Rev Lett.* 1996; 77:3865-8.
- [38] Grimme,S. Semiempirical hybrid density functional with perturbative second-order correlation. *J. Chem. Phys.* 2006; 124: 034108.
- [39] Tobias Schwabe and Stefan Grimme. Double-hybrid density functionals with long-range dispersion corrections: higher accuracy and extended applicability. *Phys. Chem. Chem. Phys.* 2007; 9: 3397-3406.
- [40] Halgren, T. A.; Lipscomb, W. N. The synchronous-transit method for determining reaction pathways and locating molecular transition states. *Chem Phys Lett*, 1977; 49(2): 225-232.
- [41] Frisch, M. J.; Trucks, G. W.; Schlegel, H. B. et al. Gaussian 09, revision D.01; Gaussian, Inc.: Wallingford, CT, 2013.
- [42] E.H. Majzoub. First-Principles Calculated Phase Diagram for Nanoclusters in the Na-Al-H System: A Single-Step Decomposition Pathway for NaAlH₄. *J. Phys. Chem. C.* 2011; 115: 2636–2643.
- [43] Christian, M.; Aguey-Zinsou, K.-F. Destabilisation of Complex Hydrides through Size Effects. *Nanoscale.* 2010; 2: 2587–2590.
- [44] Gonzalez C, Schlegel HB. An improved algorithm for reaction path following. *J. Chem Phys* 1989; 90: 2154-61.
- [45] Gonzalez C, Schlegel HB. Reaction path following in massweighted internal coordinates. *J Phys Chem.* 1990; 94: 5523-5527.
- [46] Alan E. Reed, Robert B. Weinstock, and Frank Weinhold. Natural population analysis. *J. Chem. Phys.* 1985; 83: 735.
- [47] Becke, A. D.; Edgecombe, K. E. A simple measure of electron localization in atomic and molecular systems. *J. Chem. Phys.* 1990; 92:5397–5403.
- [48] Savin, A.; Nesper, R.; Wengert, S.; Fassler, T. F. ELF: The Electron Localization Function. *Angew. Chem., Int. Ed. Engl.* 1997; 36: 1808–1831.
- [49] Dronskowski R, Bloechl PE. Crystal orbital Hamilton populations (COHP): energy-resolved visualization of chemical bonding in solids based on density-functional calculations. *J Phys Chem.* 1993; 97: 8617-24.
- [50] Steinberg S, Dronskowski R. The crystal orbital Hamilton population (COHP) method as a tool to visualize and analyze chemical bonding in intermetallic compounds. *Crystals.* 2018; 8: 225.
- [51] Deringer VL, Tchougreeff AL, Dronskowski R. Crystal orbital Hamilton population (COHP) analysis as projected from plane-wave basis sets. *J Phys Chem A.* 2011; 115. 5461-54666.